ELSEVIER

Polymer 40 (1999) 6443–6450

polymer

Rheological investigation on the anisotropic phase of cellulose–MMNO/H_2O solution system

Sang Ouk Kim[a], Won Ju Shin[a], Hansol Cho[a], Byoung Chul Kim[b], In Jae Chung[a,*]

[a]Department of Chemical Engineering, Korea Advanced Institute of Science and Technology, 373 ~ 1 Kusong, Yusong, Taejon 305 ~ 701, South Korea
[b]Division of Chemical Engineering, Hanyang University, 17 Haengdang, Seongdong, Seoul 133 ~ 791, South Korea

Received 3 August 1998; received in revised form 12 October 1998; accepted 1 December 1998

Abstract

The cellulose solutions in *N*-methyl-morpholine-*N*-oxide (MMNO)/H_2O were prepared. The cellulose concentration was varied from 5 to 25 wt.%. The mole ratio of water to MMNO was fixed at 0.8 and propyl gallate (~1 wt.%) was added as an antioxidant. To observe the anisotropic phase formation, polarized light microscopy, DSC, dynamic rotational rheometry and capillary rheometry experiments were performed. Polarized light micrographs revealed anisotropy for the cellulose solutions of 20 wt.% and higher concentrations. The anisotropy become clearer when sheared. It was difficult to detect the isotropic transition temperature and concentration from DSC and dynamic viscosity. In capillary rheometry measurements, however, both viscosity drop at the anisotropic to isotropic transition concentration and flow activation energy change at the transition temperature were observed. The phase transition temperature and concentration were 95°C–100°C and about 23 wt.%, respectively. Time–temperature superposition principle was applied successfully to the solutions below 20 wt.% concentration but failed for the solutions above 20 wt.% concentration. The largest deviation from superposition was found at 23 wt.% solution which was the critical concentration.

Keywords: Cellulose MMNO/H_2O solution; Anisotropic phase transition; Time temperature superposition

1. Introduction

Cellulose is the most abundant natural polymer source. However, its use is restricted owing to poor processibility, which originates from its infusibility and poor solubility. At present, the well known process for the production of viscose rayon is also the most widely used method to process cellulose for fiber spinning. However, this process is declining because of pollution problems associated with toxicity of solvent. Numerous researches have been carried out to develop a nontoxic and easy dissolution system of cellulose. In indirect solvent systems such as dimethyl formamide/pyridine [1], dimethyl formamide/N_2O_4 and dimethyl sulfoxide/N_2O_4 [2,3]. cellulose forms derivatives during dissolution. However, direct solvent systems such as trifluoroacetic acid/dichloromethane [4], liquid ammonia/ NH_4SCN [5], dimethyl acetamide/LiCl [6], and MMNO/ H_2O [7,8] may form complexes with cellulose but the molecular structure of cellulose doesn't change during dissolution. So, the processing procedures dealing with direct solvent are much simpler than those dealing with indirect solvent. Among them, MMNO/H_2O system has some advantages; easy dissolution process, non-toxicity of solvent system, no necessity for metal salt recovery.

The dissolution of cellulose in tertiary amine oxide was discovered first by Graenacher et al. [9] in 1939 and rediscovered by Johnson later [10]. The spinning of cellulose fiber from MMNO/H_2O solution was reported by McCorsley [11]. Then, the first commercialized fiber, Tencel was developed by Courtauls. Other processes, Lyocell by Lenzing, Cocel by KIST, Alceru by TITK, etc. are also being developed. As cellulose does not form any complex when dissolved in MMNO/H_2O solvent, the dissolution mechanism is very simple. MMNO has very strong dipole, N^+O^-, so it can directly dissolve cellulose breaking the intermolecular hydrogen bonding of cellulose. MMNO/H_2O solvent with a high water content can not dissolve cellulose because the N^+O^- dipoles of MMNO molecules are saturated by excess water, whereas the solvent with a low water content has a high melting temperature at which MMNO and cellulose are degraded [12]. Actually, the water content must be 7–15 wt.% to dissolve cellulose up to a high concentration.

Cellulose solutions are known to form the anisotropic phase in various solvent systems. For the cellulose solution in MMNO/H_2O, Chanzy et al. [13] reported the anisotropic

---

* Corresponding author.
E-mail address: chung@cais.kaist.ac.kr (I.J. Chung)

0032-3861/99/$ - see front matter
PII: S0032-3861(98)00852-0

phase formation at proper conditions; temperature must be lower than 100°C, cellulose concentration higher than 20 wt.%, and the mole ratio of water to MMNO smaller than unity. Patel, et al. [14] reported the anisotropic phase formation at the 20 wt.% cellulose concentration in trifluoroacetic acid/chlorinated alkanes solution system. The mesophase was identified as cholesteric phase. The solvent system is very toxic and may degrade cellulose. Cuculo et al. [15] reported anisotropic phase formation in liquid ammonia/NH_4SCN. An interesting result is that both cholesteric and nematic phases were observed with varying the cellulose concentration. In the solvent of 75.5 wt.% NH_4SCN, cholesteric phase was formed at 3.5 wt.% of cellulose and nematic phase at 8–16 wt.%. The cellulose solution in dimethyl acetamide/LiCl solvent system showed the anisotropic phase and the critical concentration varied with the content of LiCl [16].

The rheological study has been a useful tool for the researches on cellulose solution systems. The anisotropic phase formation regions and the fiber processing conditions were determined for various cellulose and cellulose derivative solution systems by rheological measurements [17–19]. Narvard et al. [17] investigated the anisotropic to isotropic transition temperature of cellulose MMNO/H_2O solution through the flow activation energy of each phase. The exact phase transition concentration was not determined and moreover, the degradation of cellulose was pointed out in the absence of antioxidant [18]. The present work addresses the conditions of anisotropic phase formation for cellulose MMNO/H_2O solution systems. The solvent system had the water content fixed at 11 wt.% and the cellulose solutions with various cellulose concentrations were prepared. The anisotropic to isotropic transition temperature and concentration were determined on rheological basis. The applicability of time temperature superposition principle was also examined.

2. Experimental

2.1. Materials

Cellulose was purchased from ITT Rayonier Co., whose degree of polymerization was informed to be 1180. It was dried overnight under vacuum at 70°C before use. Propyl gallate and MMNO/H_2O (50 wt./50 wt.) mixture were purchased from Aldrich Co. and used without further purification. MMNO/H_2O was stored carefully in a sealed vessel to prevent from absorbing moisture.

2.2. Solvent and solution preparation

The mixture of MMNO/H_2O (50 wt./50 wt.) was condensed to prepare the solvent with a low water content. The water content was controlled as follows; as received MMNO/H_2O (50 wt./50 wt.) solvent was distillated at 130°C under nitrogen atmosphere for about 10 h. It was solidified at room temperature and ground into fine powder in the glove box under dried nitrogen atmosphere. Then, the powder was dried in the vacuum oven with increasing temperature from 40°C to 80°C. The water content determined by NMR spectroscopy was 11 wt.% (mole ratio of H_2O to MMNO was 0.8). To prepare cellulose solutions, cellulose and solvent powder were sufficiently premixed at room temperature with 1 wt.% propyl gallate as antioxidant. This mixture was heated to 130°C in nitrogen atmosphere and stirred for about 1 h. Cellulose solutions of 5, 10, 15, 18, 20, 23 and 25 wt.% were prepared. More concentrated solution could not be obtained. All solutions were handled and stored carefully under dried nitrogen atmosphere.

2.3. Water content determination

500 MHz ^1H NMR (Bluker, AMX FT NMR spectroscopy) was used to measure the water content of dried MMNO/H_2O powder quantitatively. Deuterated DMSO was used as a solvent and the integrated areas of the water proton peaks at 3.5–3.7 ppm was compared with those of MMNO proton peaks to quantify the water content in the MMNO/ H_2O solvent.

2.4. Polarized light microscopy and thermal transition analysis

Polarized light microscope (A Leitz, Model Laborlux 12 Pols) with hot stage was used to observe the textures of cellulose solutions. A fragment of cellulose solution was squeezed between two glass slides at 80°C and then sealed for the polarized optical microscopy observation. DSC (Du Pont model 910 analyzer) was used to study the thermal transition behavior of cellulose solutions with increasing temperature at the heating rate of 5°C/min.

2.5. Rheological analysis

A capillary rheometer (Rosand RH5) was used to measure the steady shear viscosity of cellulose solutions in the temperature range of 85°C–125°C at various shear rates (30–300 s^{-1}). The capillary die with inlet angle of 180°, diameter of 0.1 mm and the ratio of length to diameter (L/D) of 16 was used. Shear rate was corrected by Rabinowitisch correction. Rotational rheometer (Physica Rheo Lab MC120) was used to measure the dynamic viscoelastic properties of cellulose solutions. Parallel plate geometry of 25 mm diameter and 0.5 mm gap size was used for all cases. Predetermined mass of bulk samples was loaded on rheometer fixture and squeezed to the gap size. To prevent the water evaporation during rheological measurement with the rotational rheometer, the edge of the sample between plates was coated with a mineral oil after the sample loading [20].

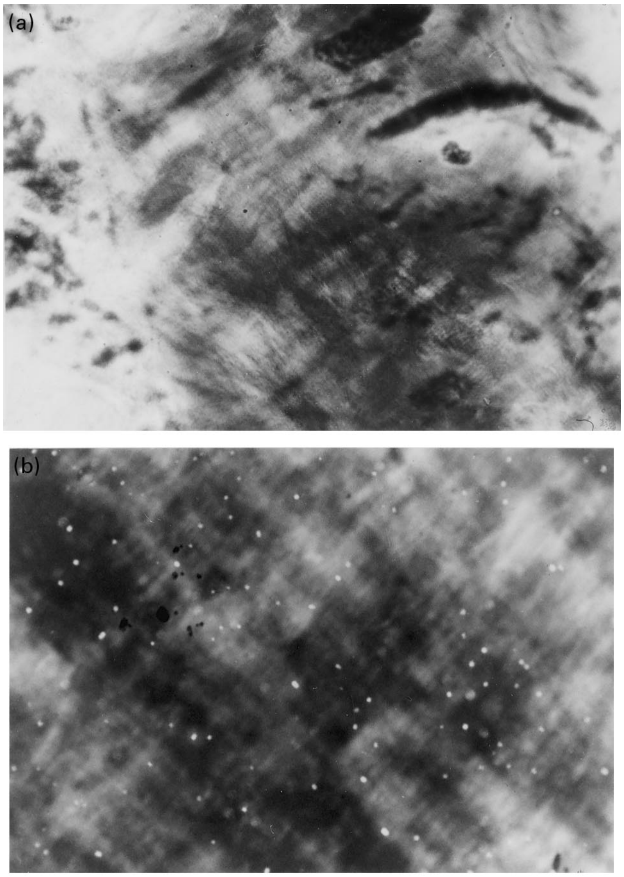

Fig. 1. Polarized light micrographs of cellulose MMNO/H_2O solutions heated to 110°C and then sheared at observed temperatures; (a) 20 wt.% solution at 85°C and (b) 25 wt.% solution at 90°C.

3. Results and discussion

3.1. Polarized light microscopy

To confirm the anisotropy formation of cellulose NMMO/H_2O solution, all prepared solutions were observed on polarized light microscopy. The strong optical anisotropy was observed for 23 and 25 wt.% cellulose solutions below 100°C. As the texture does not show distinct domains, as already reported by Chanzy, et al. [13], it is not sure whether the texture is the completely anisotropic or biphasic. Upon heating anisotropy disappeared around 100°C. Anisotropy recovery was so slow that on subsequent cooling to 85°C–90°C the anisotropy did not recover. Even after several hours of annealing at 90°C, anisotropy was relatively weak. The recovered anisotropy disappeared again around 100°C on heating. Only when the samples heat treated over 100°C were sheared below 100°C by pulling the cover glass of the samples, the strong anisotropy similar to the initially observed one reappeared. As the cellulose solutions experienced squeezing flow during sample preparation, the initial texture showed a strong anisotropy. For the case of 20 wt.% solutions, although relatively weaker than for the higher concentration solutions, anisotropy was also observed and the phase behavior with temperature variation was similar to the higher concentration ones.

The slow anisotropy evolution is some contrary to the earlier results by Chanzy, et al. [13], where they reported the complete texture recovery of cellulose–MMNO/H_2O solution during 1 °C/min cooling. The contrary may be attributed to the difference of degree of polymerization of cellulose. Chanzy et al. used the cellulose with the degree of polymerization of 35–600, half or more lower than ours. The difference of degree of polymerization may lead to the difference of molecular mobility and so phase transition kinetics. Fig. 1 shows the anisotropic textures of 20 and 25 wt.% cellulose solutions at 85°C and 90°C respectively. The samples were preheated above 110°C, cooled to the observation temperature and then sheared. The solutions with the cellulose concentration below 20 wt.% did not show any anisotropy even when sheared.

3.2. DSC

Fig. 2 shows the results of DSC experiments conducted for pure solvent and cellulose solutions. There are endotherms located between 62°C–75°C, the melting transitions of the monohydrated MMNO. In the case of pure solvent, a sharp single endothermic peak appears at 74.5°C as a single sharp peak [21]. But for the 5 wt.% cellulose solution, the melting transition is divided into two peaks, a broader one at 70.3°C and a sharper one at 74.5°C. The peak at the higher temperature is close to the melting temperature of pure monohydrated MMNO. With increasing the cellulose concentration, the positions of both peaks shift to a lower temperature and the peak areas are reduced. Above 15 wt.% concentration, the higher temperature transition almost disappears. The reduction of the transition peaks with cellulose concentration implies that the cellulose polymer chain disturbs the crystallization of the monohydrated MMNO [22]. By the way, in the temperature range between 90°C and 110°C, which involves the isotropic transition region on polarized light microscopy observation, no transition peak is detected in DSC heating curves. The same results were obtained for the samples preannealed at 80°C for 10 h.

3.3. Complex viscosity change with temperature and concentration

Whereas MMNO is very hygroscopic at room temperature, water in MMNO/H_2O system evaporates easily at a high temperature. Whatever the case is, the water content in a sample may seriously affect the rheological properties. To keep the water content constant in the sample during dynamic rheological experiments, the edge of the sample was covered with a mineral oil after loading on the rheometer fixture. Fig. 3 (a) and (b) show the variation of dynamic viscoelastic properties with time for 18 wt.% solution at 100°C and 25 wt.% at 90°C, respectively. Closed symbols stand for the samples covered with mineral oil

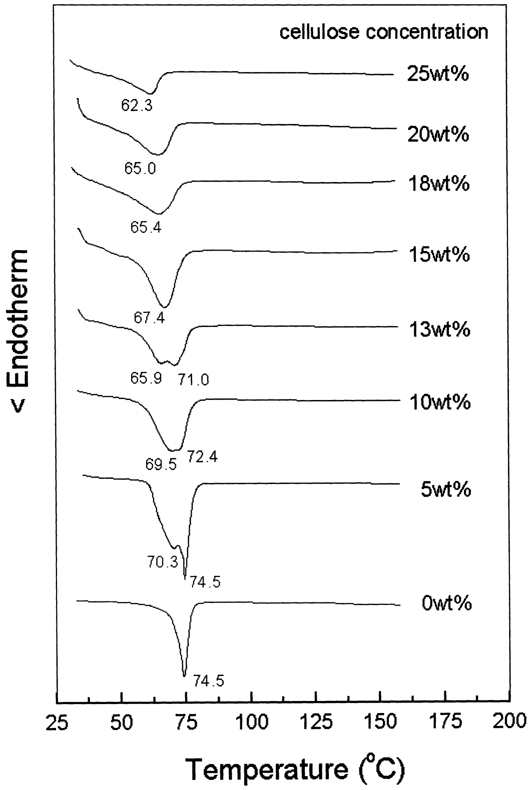

Fig. 2. DSC thermograms of MMNO/H_2O solvent and cellulose MMNO/H_2O solutions at the heating rate of 5°C/min.

and open symbols for those not covered. The deformation was 0.05 in the range of linear viscoelasticity and angular frequency was 10 rad/s. Without mineral oil coverage, the viscoelastic property values grow with time. The extent of growth is serious at a lower cellulose concentration and a high experimental temperature. We could observe white anhydrous MMNO particles on the edge of the sample after the measurements, which was ascribable to water evaporation on the edge of the sample geometry. When the sample edge was covered with a mineral oil, the viscoelastic properties sustained for about 1 h or more. The initial viscosity values for both samples covered and not covered with a oil were identical within the experimental error.

To observe the complex viscosity change in the isotropic transition region, complex viscosities of 15, 18, 20 and 25 wt.% solutions were measured by the temperature sweep tests at a heating rate of 1°C/min. The sample edge was covered with oil. As shown in Fig. 4, the complex viscosities of all concentrations do not show any noticeable change with temperature. It just decreases monotonically with temperature. Fig. 5 shows the complex viscosity change with concentration for several frequencies. Each measurements were performed in frequency sweep mode and the measured temperature was 90°C, where anisotropy was observed on polarized light microscopy for the solutions over 20 wt.% concentration. As the results of temperature sweep tests, the abrupt increase or decrease of viscosity at the phase transition is not seen. The complex viscosities just increase with concentration.

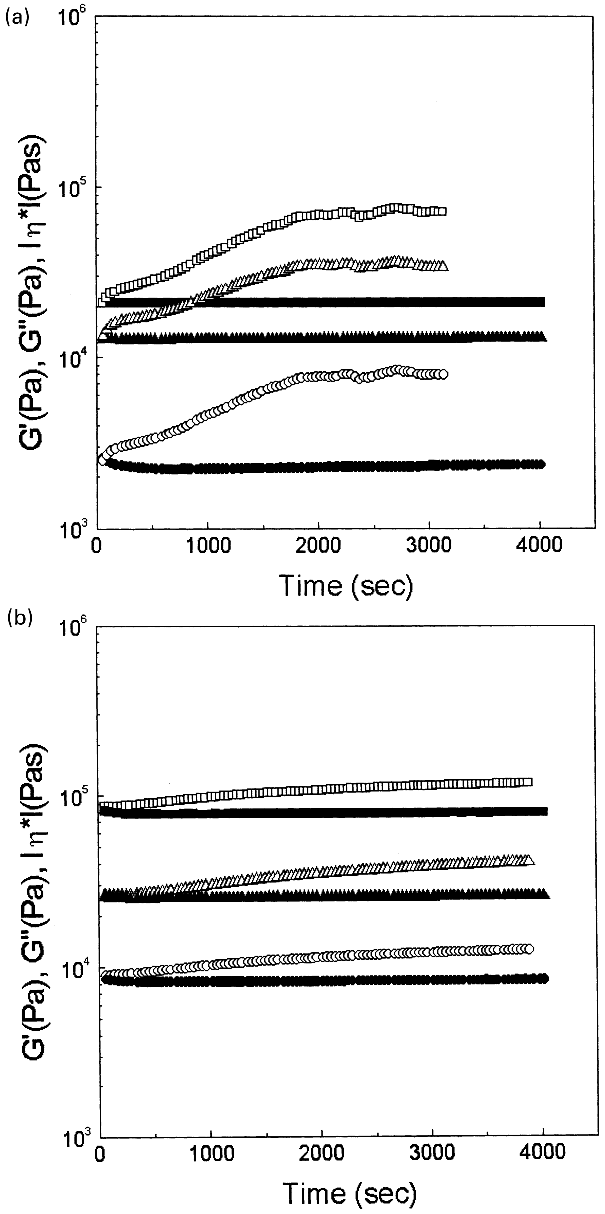

Fig. 3. Variations of viscoelastic properties with time for cellulose MMNO/H_2O solutions with oil coverage [closed symbols: (■) G′; (▲) G″; (●) $|\eta^*|$] and without oil coverage [open symbols: (□) G′; (△) G″; (○) $|\eta^*|$]; (a) 18 wt.% solution at 100°C and (b) 25 wt.% solution at 90°C. $\omega = 10$ rad/s. $\gamma = 0.05$.

3.4. Capillary rheometry

From the hint that cellulose shows clearer anisotropy under shear in the polarized light microscopy observation, the capillary rheometry measurements were performed, which was also suggested by Navard et al., as a tool to determine the anisotropic–isotropic transition temperature of a cellulose solution [17]. The experiments were done in

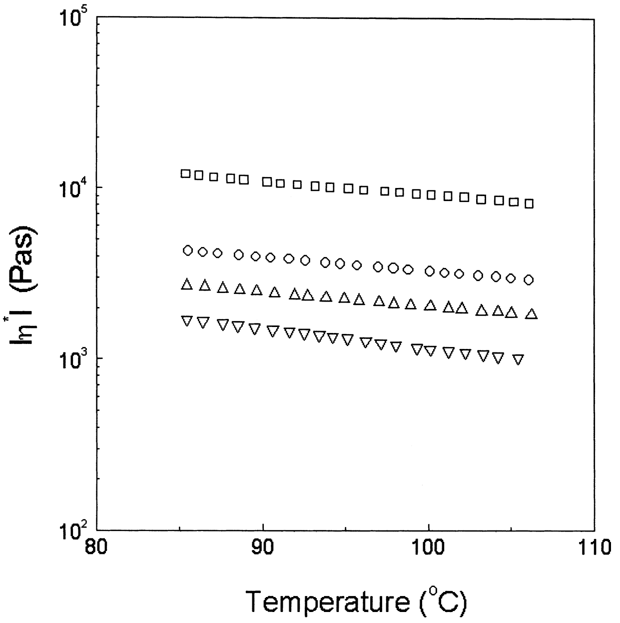

Fig. 4. Temperature dependence of complex viscosity, $|\eta^*|$ for cellulose MMNO/H_2O solutions of various concentrations at the heating rate of 1°C/min: (□) 25 wt.%; (○) 20 wt.%; (△) 18 wt.%; (▽) 15 wt.%. $\omega = 10$ rad/s. $\gamma = 0.05$.

shear rate sweep mode. To insure the reproducibility of obtained data, the measurements were done four times in twice successive heating and cooling cycles for each temperature. The results showed good reproducibility for all cases.

Fig. 6 shows the concentration dependence of apparent viscosity. Above 100°C the apparent viscosity increases monotonically with concentration. On the contrary, below 100°C the viscosity increases rapidly between 20 and 23 wt.% concentrations and then suddenly drop to a lower value between 23 and 25 wt.%. Such behavior is a clear evidence of isotropic to anisotropic phase transition [23]. From these results the isotropic to anisotropic phase transition occurs around 23 wt.% concentration.

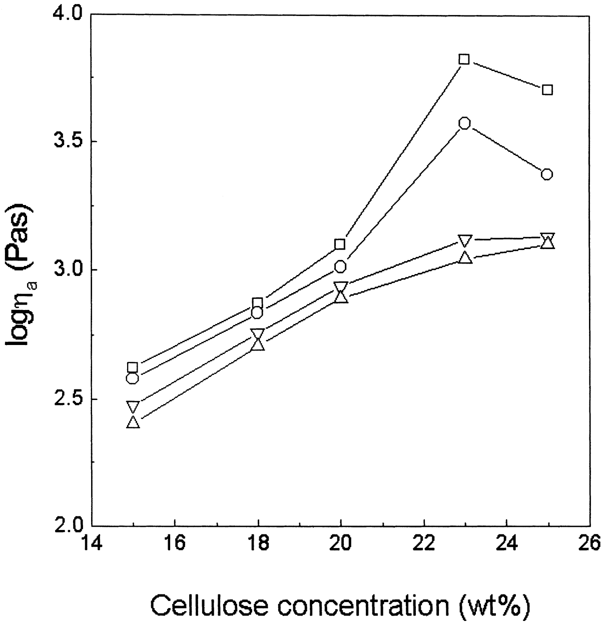

Fig. 6. Concentration dependence of apparent viscosity, η_a for cellulose MMNO/H_2O solutions at various temperatures: (■) 85°C; (●) 90°C; (▼) 100°C; (▲) 110°C. $\dot{\gamma} = 50\ \mathrm{s}^{-1}$. All viscosity values were Rabinowitisch corrected.

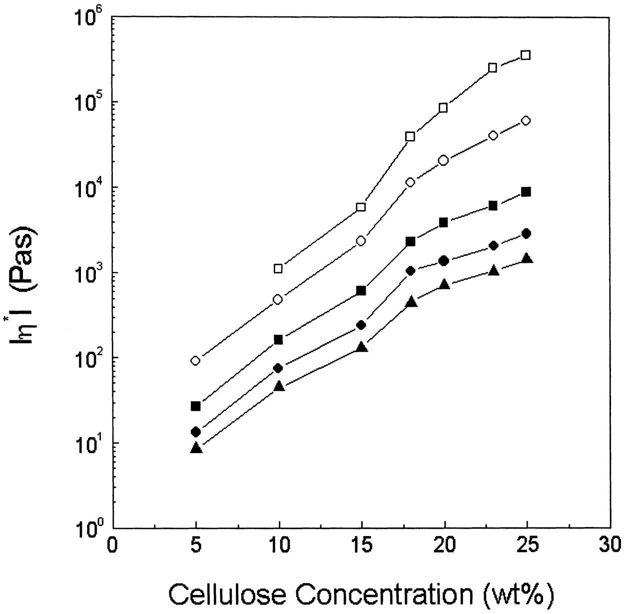

Fig. 5. Concentration dependence of complex viscosity, $|\eta^*|$ for cellulose MMNO/H_2O solutions at 90°C: (□) 0.1 rad/s; (○) 1.3 rad/s; (■) 12.9 rad/s; (●) 46.5 rad/s; (▲) 100 rad/s. $\gamma = 0.05$.

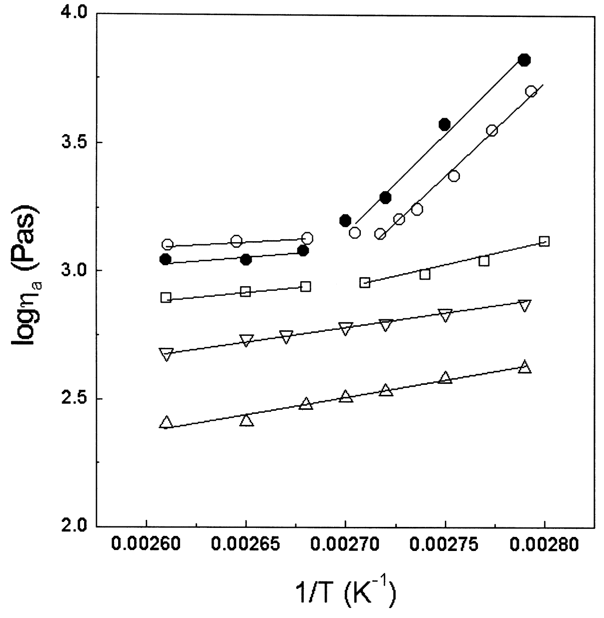

Fig. 7. Arrhenius type plot of apparent viscosity, η_a for cellulose MMNO/H_2O solutions: (○) 25 wt.%; (●) 23 wt.%; (□) 20 wt.%; (▽) 18 wt.%; (△) 15 wt.%. $\dot{\gamma} = 50\ \mathrm{s}^{-1}$. All viscosity values were Rabinowitisch corrected.

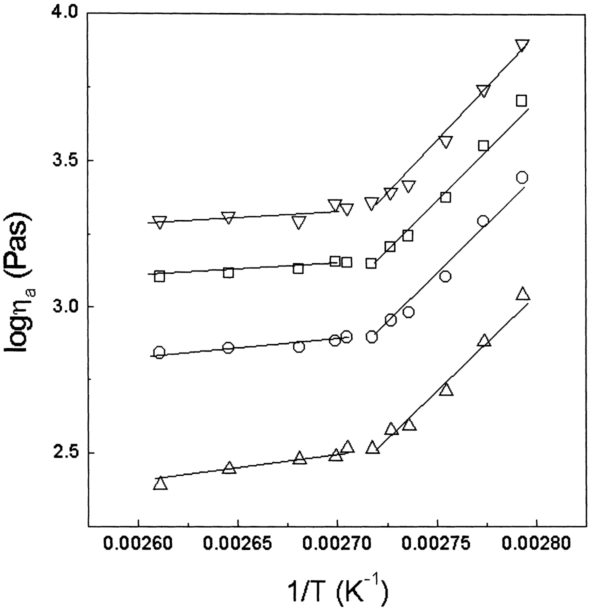

Fig. 8. Arrhenius type plot of apparent viscosity, η_a of 25 wt.% cellulose MMNO/H_2O solutions at various shear rates: (▼) 30 s^{-1}; (■) 50 s^{-1}; (●) 100 s^{-1}; (▲) 300 s^{-1}. All viscosity values were Rabinowitisch corrected.

Meanwhile, the phase status of 25 wt.% concentration solution is still unknown. To know it, the experimental data for more concentrated solutions are necessary. However, we could not prepare higher concentration solution than 25 wt.% solution.

In order to demonstrate the isotropic transition temperature precisely, the apparent viscosities were plotted in Arrhenius form. Fig. 7 shows the results of all solutions at the shear rate of 50 s^{-1}. The 15 and 18 wt.% solutions show linear curves, which means the invariance of the flow activation energy and thus no phase transition. In 20 wt.% solutions, which show an anisotropy, there are changes in the flow activation energy between 95°C and 100°C. There are more distinct changes for 23 and 25 wt.% solution. Above 100°C, these high concentration solutions show almost the same temperature dependence as the low concentration solutions. Under 95°C, however, they show quite a different temperature dependence. Fig. 8 shows the Arrhenius type plot of apparent viscosity of 25 wt.% solution at various shear rates. The shear rate is in the range of 30–300 s^{-1}. The anisotropic to isotropic phase transition temperature region does not change with shear rate. It is in the range of 95°C–100°C for all shear rates, which agrees well with the polarized light microscopy observation. In the isotropic phase transition temperature region, cellulose solution does not show the viscosity peak shape differently from most liquid crystalline polymers. Similar results were reported for several cellulose and cellulose derivative solution systems [16,19,24].

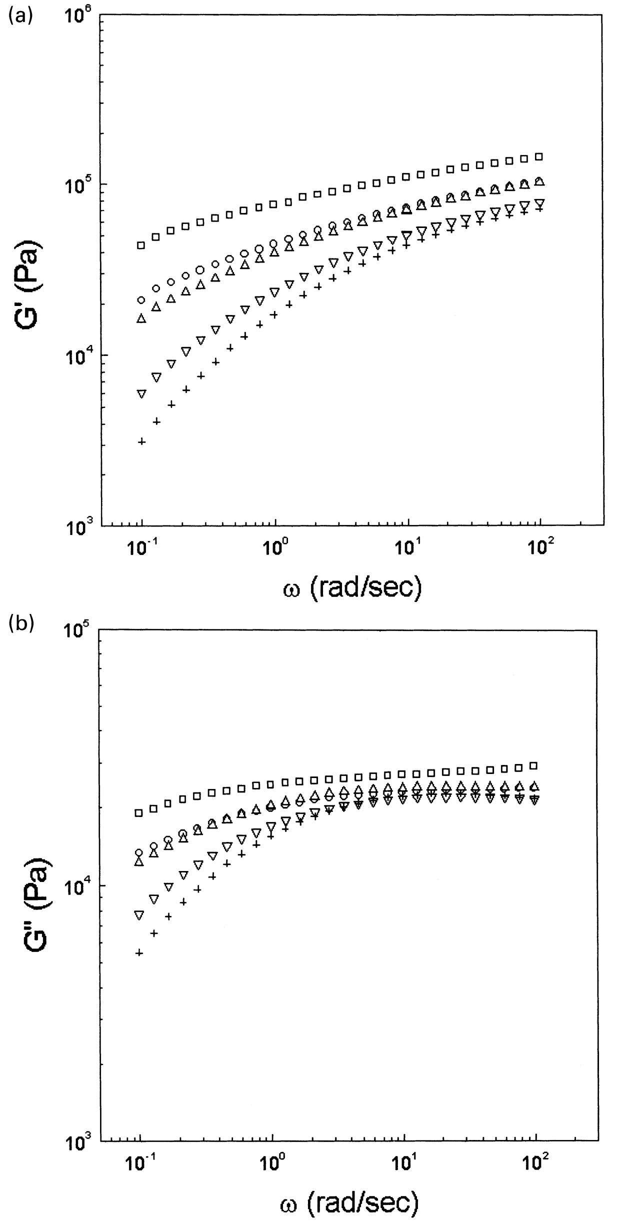

Fig. 9. Angular frequency dependence of (a) storage modulus, G′ and (b) loss modulus, G″ for 23 wt. % cellulose MMNO/H_2O solutions at various temperatures: (□) 85°C; (○) 90°C; (△) 95°C; (▽) 100°C; (+) 110°C. $\gamma = 0.05$.

3.5. Time temperature superposition

Time temperature superposition was tested around the isotropic phase transition temperature region. It is known that the polymer system in anisotropic or biphasic state does not follow time temperature superposition principle [25–27]. Fig. 9(a) and (b) are the storage and loss moduli of 23 wt.% solutions at various temperatures. Similar to the results of the complex viscosity change with temperature, the moduli just decrease with temperature over the measured frequencies. From these data, time temperature superposition was conducted. The reference temperature

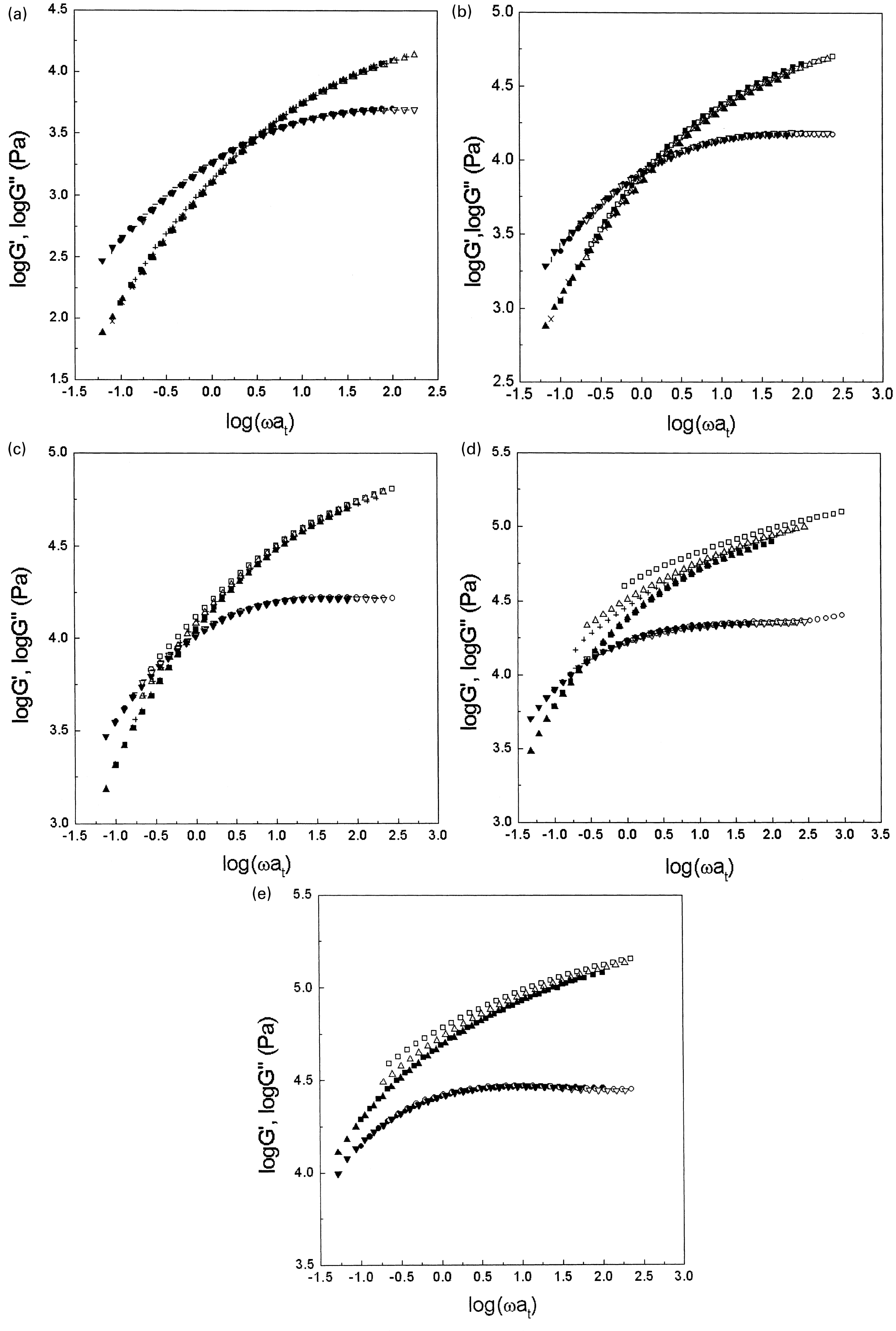

Fig. 10. Time temperature superposition results of storage moduli, G', and loss moduli, G' for cellulose MMNO/H_2O solutions of (a) 15 wt.%, (b) 18 wt.%, (c) 20 wt.%, (d) 23 wt.%, and (e) 25 wt.% concentration: (■) G' and (●) G'' at 100°C; (□) G' and (○) G'' at 85°C; (△) G' and (▽) G'' at 90°C; (() G' and (−) G'' at 95°C; (×) G' and (|) G'' at 105°C; (▲) G' and (▼) G'' at 110°C.

was 100°C. Both moduli and frequencies were shifted empirically. As proposed by Hudson, et al. for the anisotropic polymers, loss moduli were superposed ahead as a standard [25,26].

For 15 and 18 wt.% solutions the time and temperature superpose very well for all tested temperatures as shown in Fig. 10(a) and (b). The same result was reported for 12 wt.% cellulose MMNO/H_2O solution [28]. This superposition indicates that low concentration cellulose solutions are in the isotropic state. However, time temperature superposition principle fails for the solutions above 20 wt.% concentration. Fig. 10(c) and (d) illustrate the results. Although the loss moduli are superposed, the elastic moduli are not superposed below 100°C. The failure of time temperature superposition means nonhomogeneity of the polymer solution system. Such nonhomogeneity in polymer solution system can be originated from several kinds of reasons such as solid formation, micro phase separation [29], and anisotropic phase formation [25–27]. In general, the solid formation and liquid liquid transition such as micro phase separation and gelation become more pronounced as the concentration increases. In those cases, deviation from the superposition gets larger with concentration. As shown in Fig. 10(d), however, the cellulose solutions shows the largest deviation of storage moduli at the concentration of 23 wt.%, which showed the maximum apparent viscosity value in capillary rheometry study. So the anisotropic phase formation is the reason for the failure of time temperature superposition and the largest deviation of storage modulus at 23 wt. % can be another evidence of biphasic nature at this concentration. Hudson, et al. reported that the largest deviation of storage modulus was obtained in the smectic to nematic phase transition region for a thermotropic polymer [26]. They did not perform time temperature superposition in anisotropic to isotropic phase transition temperature region.

4. Conclusion

We investigated the phase behavior of cellulose MMNO/H_2O solution system by rheological methods. Cellulose solutions of concentration between 5–25 wt.% are prepared. The water content in the solvent was 11 wt.% and antioxidant was used to prevent the degradation of cellulose. Polarized light microscopy revealed an anisotropy for the solutions over 20 wt.% concentration and the isotropic phase transition around 100°C. The anisotropic phase formation was activated when the external shear flow was applied. However, it was difficult to detect the phase transition temperature from DSC and dynamic temperature sweep measurements. The phase transition region was determined by using a capillary rheometer. The critical concentration was found to be around 23 wt.% over which the apparent viscosity abruptly dropped. The phase transition temperature determined from the changes of flow activation energy was 95°C to 100°C. Time temperature superposition was applied successfully to the solutions below 20 wt.% concentration but failed for those solutions above 20 wt.%. The largest relative deviation from superposition was found at 23 wt.%, which was the critical concentration as shown in the capillary rheometer experiments.

References

[1] Kamide K, Okajima K, Matsui T, Manabe S. Polym J (Tokyo) 1980;12:521.

[2] MacDonald DM. In: Turbak AF, editor. Solvent spun rayon, modified cellulose fibers and derivatives. Washington DC: American Chemical Society, 1977. p. 25–39.

[3] Hummer RB, Turbak AF. In: Turbak AF, editor. Solvent spun rayon, modified cellulose fibers and derivatives. Washington DC: American Chemical Society, 1977. p. 44–51.

[4] Khripunov AK, Pliski EA, Laius LA, Baklagina YuG, Petrova VV, Gerasimova VA. Vysokomol S edin B 1975;17:600.

[5] Scherer P. J Am Chem Soc 1931;53:4009.

[6] McCormick CL. US Patent 4,278,790, 1981.

[7] Franks NE, Varga SK. US Patent 4145532, 1979.

[8] Turbak AF, Hammer RB, Davies RE, Hergert HT. Chem Techno 1977;11:702.

[9] Graenacher G, Sallmann R. US Patent 2179181, 1939.

[10] Johnson DL. Brit Patent 1144048, 1967.

[11] McCorsley CC. US Patent 4246221, 1981.

[12] Chanzy H, Nawrot S, Peguy A, Smith P. J Polym Sci Poly Phys Ed 1982;20:1909.

[13] Chanzy H, Peguy A, Chaunis S, Monzie P. J Polym Sci Polym Phys Ed 1980;18:1137.

[14] Patel DL, Gilbert RD. J Polym Sci Polym Phys Ed 1981;19:1231.

[15] Yang KS, Theil MH, Cuculo JA. In: El Nokaly MA, editor. Polymer association structures. Washington DC: American Chemical Society, 1989, ACS Symposium Series No. 384, p. 156–183.

[16] McCormick CL, Callais PA, Hutchinson Jr BH. Macromolecules 1985;18:2394.

[17] Navard P, Haudin JM. Br Polym J 1980;12:174.

[18] Navard P, Haudin JM. Polym Proc Eng 1985;3:291.

[19] Dave V, Glasser WG. J Appl Polym Sci 1993;48:683.

[20] Frey MW, Cuculo JA, Khan SA. J Polym Sci Polym Phys Ed 1996;34:2375.

[21] Chanzy H, Nawrot S, Peguy A, Smith P, Chevalier J. J Polym Sci Polym Phys Ed 1982;20:1909.

[22] Chanzy H, Dube M, Marchessault RH. J Polym Sci Polym Lett Ed 1979;17:219.

[23] Kiss G, Porter RS. J Polym Sci Polym Phys Ed 1980;18:361.

[24] Hong YK, Hawkinson DE, Kohout E, Garrard A, Fornes RE, Gilbert RD. In: Polymer association structures. Washington DC: American Chemical Society, 1989, ACS Symposium Series No. 384, p. 184–203.

[25] Hudson SD, Lovinger AJ, Larson RG, Davis DD, Garay RO, Fujishiro K. Macromolecules 1993;26:5643.

[26] Alt DJ, Hudson SD, Garay RO, Fujishiro K. Macromolecules 1995;28:1575.

[27] Chang S, Han CD. Macromolecules 1997;30:1656.

[28] Schrempf C, Schild G, Ruf H. Papier 1995;49:748.

[29] Han CD, Kim J. J Polym Sci Polym Phys Ed 1987;25:1741 and references therein.